This article was downloaded by:
On: *23 January 2011*
Access details: *Access Details: Free Access*
Publisher *Taylor & Francis*
Informa Ltd Registered in England and Wales Registered Number: 1072954 Registered office: Mortimer House, 37-41 Mortimer Street, London W1T 3JH, UK

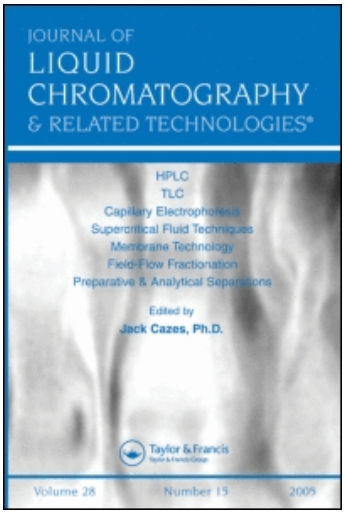

Journal of Liquid Chromatography & Related Technologies

Publication details, including instructions for authors and subscription information:
http://www.informaworld.com/smpp/title~content=t713597273

On the Precision of Particle Size Analysis by Micro-Thermal Field-Flow Fractionation

Věra Kašpárková[a]; Věra Halabalová[a]; Lubomír Šimek[a]; Jiří Dostál[a]; Josef Janča[b]
[a] Faculty of Technology, Tomas Bata University, Zlín, Czech Republic [b] Pôle Sciences et Technologie, Université de La Rochelle, La Rochelle, France

To cite this Article Kašpárková, Věra , Halabalová, Věra , Šimek, Lubomír , Dostál, Jiří and Janča, Josef(2006) 'On the Precision of Particle Size Analysis by Micro-Thermal Field-Flow Fractionation', Journal of Liquid Chromatography & Related Technologies, 29: 19, 2771 — 2786
To link to this Article: DOI: 10.1080/10826070600958858
URL: http://dx.doi.org/10.1080/10826070600958858

PLEASE SCROLL DOWN FOR ARTICLE

Full terms and conditions of use: http://www.informaworld.com/terms-and-conditions-of-access.pdf

This article may be used for research, teaching and private study purposes. Any substantial or systematic reproduction, re-distribution, re-selling, loan or sub-licensing, systematic supply or distribution in any form to anyone is expressly forbidden.

The publisher does not give any warranty express or implied or make any representation that the contents will be complete or accurate or up to date. The accuracy of any instructions, formulae and drug doses should be independently verified with primary sources. The publisher shall not be liable for any loss, actions, claims, proceedings, demand or costs or damages whatsoever or howsoever caused arising directly or indirectly in connection with or arising out of the use of this material.

Journal of Liquid Chromatography & Related Technologies®, 29: 2771–2786, 2006
Copyright © Taylor & Francis Group, LLC
ISSN 1082-6076 print/1520-572X online
DOI: 10.1080/10826070600958858

On the Precision of Particle Size Analysis by Micro-Thermal Field-Flow Fractionation

Věra Kašpárková, Věra Halabalová, Lubomír Šimek, and Jiří Dostál
Faculty of Technology, Tomas Bata University, Zlín, Czech Republic

Josef Janča
Pôle Sciences et Technologie, Université de La Rochelle, La Rochelle, France

Downloaded At: 17:59 23 January 2011

Abstract: Micro-Thermal Field-Flow Fractionation of polymer colloidal particles was performed in two different laboratories. Short term repeatability of the experimental retentions obtained in a single laboratory has been found to be very high. The short term precision (expressed as percent standard deviation) of the determination of average particle diameter can reach the values greater than 1%, relative. Average repeatability of the retentions in both laboratories was better than 3%, relative when using identical experimental protocol. No other method of particle size analysis can provide the results of a comparable precision. Average repeatability of the width of the raw fractograms, which contains the information on particle size distribution, is of the order of 5%, relative. However, this value cannot be considered as the ultimate limit because the experiments were not carried at the low flow rate of the carrier liquid permitted to reach much higher resolution. The effect of the stability of the most important operational variables, such as the temperature drop between the cold and hot walls, the temperature of the cold wall, and the flow rate of the carrier liquid, on the precision of the analytical results is discussed.

Keywords: Micro-thermal field-flow fractionation, Analysis, Repeatability, Reproducibility, Colloidal particles

This article is dedicated to the memory of J. C. Giddings (1930–1996)

Address correspondence to Josef Janča, Pôle Sciences et Technologie, Université de La Rochelle, Avenue Michel Crépeau, 17042 La Rochelle, France. E-mail: jjanca@phys.univ-1r.fr

INTRODUCTION

Very soon after the appearance of the paper by Giddings,[1] announcing just 40 years ago the concept of Field-Flow Fractionation (FFF), the oldest of all FFF methods, Thermal Field-Flow Fractionation (TFFF), has been implemented experimentally and applied to the separation of polystyrenes.[2] Although this implementation was already published in 1967 and the first extension of the application of TFFF to other synthetic polymers was performed in 1979,[3] the repeatability of the measurements determining the precision of the method has never been studied systematically. Nevertheless, such a study has a crucial importance in the investigation of the mechanism of thermal diffusion and secondary effects since, very often, the differences in experimental results published by different authors are just on the limit of the presumed repeatability of the separation. Moreover, the TFFF can seriously be compared with other competitive methods only if the precision of the analysis is objectively evaluated. Such a kind of analysis has already been performed for Size-Exclusion chromatography or other techniques of liquid chromatography used for the determination of molar mass of synthetic polymers.[4,5] The analyses were usually carried out under the recommended optimum experimental conditions and, thus, the results have been interpreted in terms of method viability and performances.

Micro-Thermal Field-Flow Fractionation (micro-TFFF) is a new, high performance separation method,[6] applicable to the analysis of particle size of the colloidal sub-micrometer and micrometer-sized particles of the synthetic, natural, or biological origin. It has already been proven experimentally[7] that the high resolution in the analysis of the colloidal particles by micro-TFFF is achieved facilely because the manipulation of the operational variables is very easy and, thus, the optimum experimental conditions can be established for each particular case. However, until now, no systematic study was carried out concerning the repeatability of the measurements that determine the precision of the results in particle size analysis (PSA). Quite surprisingly, although several experimental studies of thermal diffusion behavior of the colloidal particles have been published with the use of standard size TFFF channels (see, e.g., ref.[8–12] and the publications cited therein), the investigation of the viability of such measurements was not at all carried out. In this paper, the micro-TFFF experiments performed in two different laboratories, and oriented towards the determination of the precision of the analysis of particle size distribution (PSD) and average particle size of well characterized polymer latex standards are described.

THEORY

The retention ratio describing the simultaneous action of the polarization (normal) and steric exclusion mechanisms is:[13]

$$R = 6(\alpha - \alpha^2) + 6\lambda(1 - 2\alpha)\left[\coth\left(\frac{1 - 2\alpha}{2\lambda}\right) - \frac{2\lambda}{1 - 2\alpha}\right] \qquad (1)$$

Downloaded At: 17:59 23 January 2011

where $\alpha = r/w$ is the ratio of the radius of the separated species to the thickness of the separation channel and λ is a dimensionless retention parameter defined below. Whenever α approaches zero, the polarization mechanism prevails and Eq. (1) takes its usual truncated form:

$$R = 6\lambda\left[\coth\left(\frac{1}{2\lambda}\right) - 2\lambda\right] \tag{2}$$

The physical meaning of the retention ratio can clearly be seen from the following equation which is based on the experimental data:

$$R = \frac{V_0}{V_R} = \frac{t_0}{t_R} \tag{3}$$

where V_0 and t_0 are retention volume and retention time of the non-retained species, respectively, and V_R and t_R are retention volume and retention time of the retained species, respectively. For highly retained species, Eq. (2) reduces to:

$$\lim_{\lambda \to 0} R = 6\lambda \tag{4}$$

The elution order in polarization FFF is usually from the small to the large species but it is inverted in purely steric exclusion mode. Consequently, an optimum thickness of the micro-TFFF channel must be carefully chosen in order to avoid the undesirable simultaneous action of steric exclusion and polarization mechanisms, which results in deterioration of the resolution.[14,15]

The retention parameter λ is given by:[13]

$$\lambda = \frac{D}{D_T \Delta T} \tag{5}$$

where D is diffusion coefficient, D_T is the coefficient of thermal diffusion, and ΔT is temperature drop across the micro-TFFF channel. The colloidal particles can be considered as hard, non-interacting spheres for which the Eq. (5) can be modified by using the well known Stokes–Einstein relationship:

$$D = \frac{k_B T}{3\pi\eta d_p} \tag{6}$$

to obtain:

$$\lambda = \frac{k_B T}{3\pi\eta d_p D_T \Delta T} \tag{7}$$

where k_B is the Boltzmann constant, T is the temperature, η is the viscosity of the carrier liquid, and d_p is the particle diameter.

Equations (1, 2, 4), and (7) are rigorously valid only if the isoviscous, parabolic flow velocity profile is formed inside the channel. Such a condition is not fulfilled in micro-TFFF because the viscosity varies with the temperature across the channel. The coefficient D_T can also be temperature

Downloaded At: 17:59 23 January 2011

dependent. Nevertheless, the errors resulting from the approximate Eqs. (1, 2, 4), and (7) are negligible for highly retained species.[16]

It follows from Eq. (7) that for the given experimental conditions, namely for the temperature of the cold wall (at which the particles are usually accumulated) and given temperature drop, the dependence $\lambda\Delta T/T$ versus $1/d_p$ should be linear. This linearity, predicted by Eq. (7), was experimentally confirmed.[7,17] Consequently, the dependence of $\lambda\Delta T/T$ on $1/d_p$ can be used as a calibration function applicable for the calculations of the particle size distribution and average particle size of an unknown sample of the colloidal particles of the same chemical nature as the particles used to establish the calibration plot. As a matter of fact, the dependence of the magnitude and perhaps of the sign of D_T on the properties of the colloidal particles (such as the chemical character of the surface) suspended in a given carrier liquid is not yet theoretically well understood. However, the same D_T can fairly be expected if the micro-TFFF is carried out under the same experimental conditions (including the composition of the carrier liquid) applied for the calibration standard samples and for chemically identical analyzed samples as well. For the identical T and ΔT, the calibration function reduces to a simple relationship:

$$\lambda = \frac{C}{d_p} \tag{8}$$

with the empirically found constant C. By combining the Eqs. (3, 4), and (8), an approximate relationship between the experimentally determined V_R and d_p can be used:

$$V_R = C' d_p \tag{9}$$

where C' is another empirical constant.

With regard to Eqs. (3, 4, 7, 8), and (9), the precision of the d_p, determined from the experimental V_R or t_R data with the use of a calibration function (Eq. 8 or 9), will be given by the repeatability of the V_R or t_R and influenced by the stability of the main experimental variable, ΔT. The absolute temperature T in Eq. (7) can be identified with the temperature of the wall at which the retained species are accumulated, usually the cold wall temperature, T_c, whose variation of even ± 2 K will obviously be less than 1%, relative of T_c. As a result, if the measurements of the V_R or the stability of the flow rate in the case of the measurements of t_R and the stability of ΔT will be better than 1%, the precision of the determined d_p could, theoretically, be better than 1%, relative.

EXPERIMENTAL

Two experimental setups for micro-TFFF (working in participating laboratories at UTB[a] and ULR[b]) onsisted of a syringe pump model IPC 2050

Downloaded At: 17:59 23 January 2011

(Linet Compact, Czech Republic) equipped with a special stainless steel syringe (Institute of Scientific Instruments, Academy of Sciences of the Czech Republic), a commercialized micro-TFFF channel unit (MicroFrac Laboratory, microfrac@atlas.cz & www.watrex.cz, Czech Republic), equipped with the electronic devices (MicroFrac Laboratory, Czech Republic) regulating the electric power for heating the cartridge and controlling the temperature of the hot wall. The dimensions of the micro-TFFF channels used in this work were $0.1 \times 3.2 \times 76$ mm. The compact micro-TFFF units were further equipped with an injection valve model 7413[a] (Rheodyne, USA) or 7410[b] with a 1 μL loop and with a system of a graduated microsplitter valve, model P 470 and a micrometering valve, model P 446 (Upchurch Scientific, USA), allowing the splitting of the carrier liquid flow into two separated entries of the channel and also the casual splitting of the outgoing liquid between the detector and the waste.[18]

A variable wavelength detector (Watrex[a] UVD 250, Czech Republic) or (Jasco[b] UV-975, Japan) equipped with 1 μL measuring cell and a PC[a] or recorder-integrator[b] (Hewlett-Packard 3395, USA) were used to record the fractograms. A low temperature thermostat model Ministat 125[a] (Huber, Germany) or RML 6 B[b] (Lauda, Germany) were used to control the temperature of the cold wall of the channel. The temperatures at very close proximities of the cold and hot walls were also measured independently by digital thermometers (GMH 3230, Greisinger electronic GmbH[a], Germany) or (Hanna Instruments[b], Portugal) equipped with two thermocouples.

A Quasi-Elastic Light Scattering (QELS) apparatus (Model Zetamaster, Malvern Instruments, U.K.) was used to check the average particle size of the studied polystyrene latex (PSL) particles in water or in the carrier liquid used in micro-TFFF.

An aqueous solution of 0.1% detergent Brij 78 (Fluka, Germany) and 3 mM NaCl was used as a carrier liquid. Spherical PSL particles (Polymer Laboratories, Great Britain) of narrow PSD and the pure acetone (non-retained marker molecules) were used in this study. The particle size of the PSL samples provided by the manufacturer and checked by QELS measurements are given in Table 1.

RESULTS AND DISCUSSION

The temperature drop, $\Delta T = 30$ K, across the channel, the temperature of the cold wall, $T_c = 303$ K, and the flow rate of 10 μL/min were chosen as optimal with regard to the acceptable resolution and separation time, found in our previous study.[7] The first experiments were aimed to determine the calibration plot (Eq. (8) with the use of all four PSL standards. The result is shown in Figure 1. The comparison of this calibration plot with our previous results (Figure 6 in ref. 17) obtained for various temperature drops ΔT indicates good agreement of the recent and previous[17] experimental

Downloaded At: 17:59 23 January 2011

Table 1. Average particle diameters of the polystyrene latex standards

Polystyrene latex sample	Average particle diameter (d_p, nm) supplier's data	Average particle diameter (d_p, nm) QELS measurements
PSL 60	60	63
PSL 108	108	105
PSL 155	155	156
PSL 343	343	350

data measured on different micro-TFFF apparatuses. The λ values were calculated from the experimental retentions R Eq. (3) by using the transcendental Eq. (2) and by applying the numerical iterations protocol. Some of the fractograms used to construct the calibration plot in Figure 1 are shown in Figure 2. The differences between the fractograms obtained in two laboratories are obviously negligible.

For the test of the repeatability, two PSL standards of particle diameter 108 nm (PSL 108) and 155 nm (PSL 155) were chosen, whose retentions lie in the central part of the calibration plot in Figure 1. The separations were carried out in two participating laboratories under identical experimental conditions (given in Experimental Section). More than ten separations of each PSL 108 and PSL 155 were performed to evaluate the repeatability of the measurements in each laboratory. Some of the fractograms are shown in Figure 3 for PSL 108 and in Figure 4 for PSL 155. The "best looking" fractograms were chosen for the PSL 108 standard and the "worst looking"

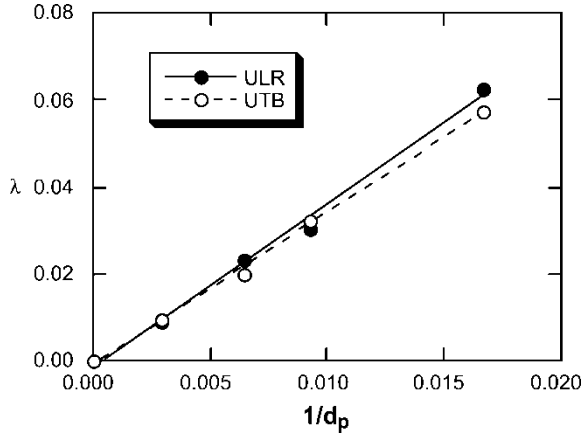

Figure 1. Calibration plot $\lambda = f(1/d_p)$ obtained for four PSL standards under the identical experimental conditions in the laboratories of UTB[a] and ULR[b] participating in the test.

Downloaded At: 17:59 23 January 2011

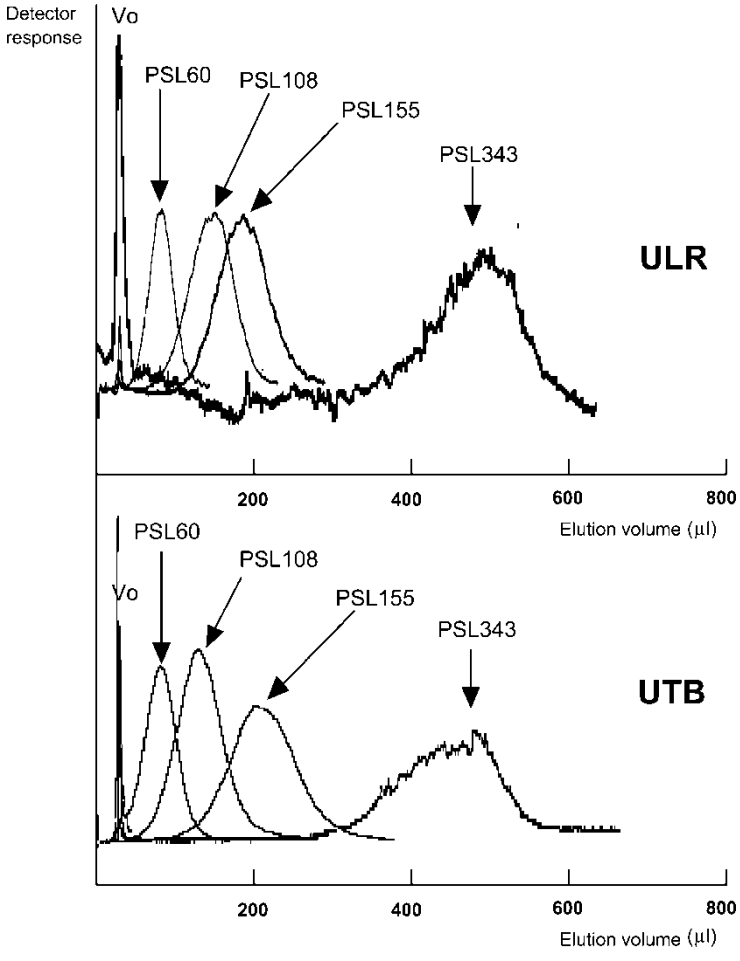

Figure 2. Fractograms of the polystyrene latexes obtained in both participating laboratories and used for the construction of the calibration plot in Figure 1.

fractograms were chosen for the PSL 155 standard, shown in Figure 3 and Figure 4, respectively. A short term stability of the detector baseline and, consequently, the noise of the detector signal represent the main difference between the "best" and "worst" fractograms. A progressive deterioration of the signal noise was observed in the course of consecutive separations performed without cleaning the channel and without using the freshly prepared carrier liquid. The cleaning of the channel was carried out by applying a very high flow rate of the deionized water used as the carrier liquid and without the application of the temperature drop. The experimental results obtained in both laboratories for PSL 108 and PSL 155 are summarized in Table 2.

Downloaded At: 17:59 23 January 2011

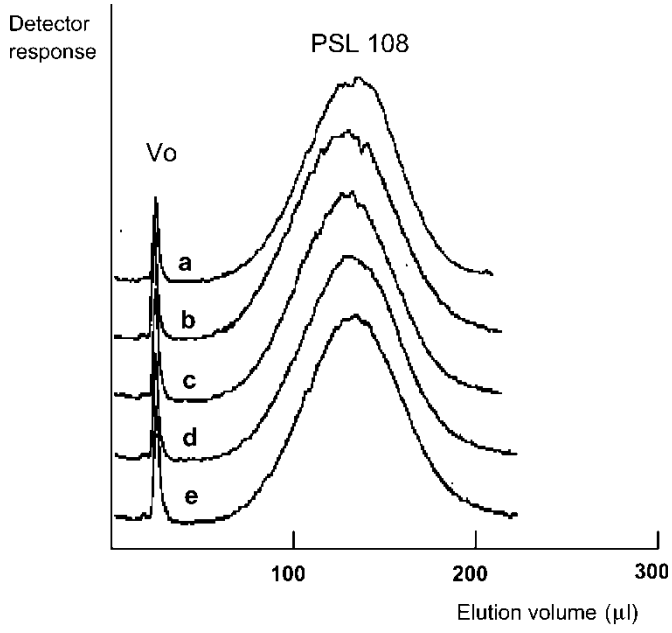

Figure 3. Five of ten fractograms of the polystyrene latex PSL 108 obtained in the laboratory of ULR[b].

The retention ratio R_{max} for each separation was determined from the experimental retention volume of the maxima of the unretained ($V_{0,max}$) and retained ($V_{R,max}$) species:

$$R_{max} = (V_{0,max}/V_{R,max}) \tag{10}$$

The mean retention ratios $\bar{R}$, resulting from the separations performed in each participating laboratory were calculated as the mean values for PSL 108 and PSL 155 standards:

$$\overline{R} = \frac{\sum_1^n \left(V_{0,max}/V_{R,max}\right)}{n} \tag{11}$$

The $\bar{R}$ values were used to calculate the $\bar{\lambda}$ from Eq. (2), as described above. The normalized width of each fractogram, expressed as normalized standard deviation, σ_N, was calculated from:

$$\sigma_N = \left(\frac{\sum_1^n (V_i/V_{0,max} - 1/\overline{R})^2 h_i}{\sum_1^n h_i}\right)^{0.5} \tag{12}$$

where V_i and h_i are the elution volume and the height of the fractogram at this elution volume, respectively, within the elution range of the retained PSL

Downloaded At: 17:59 23 January 2011

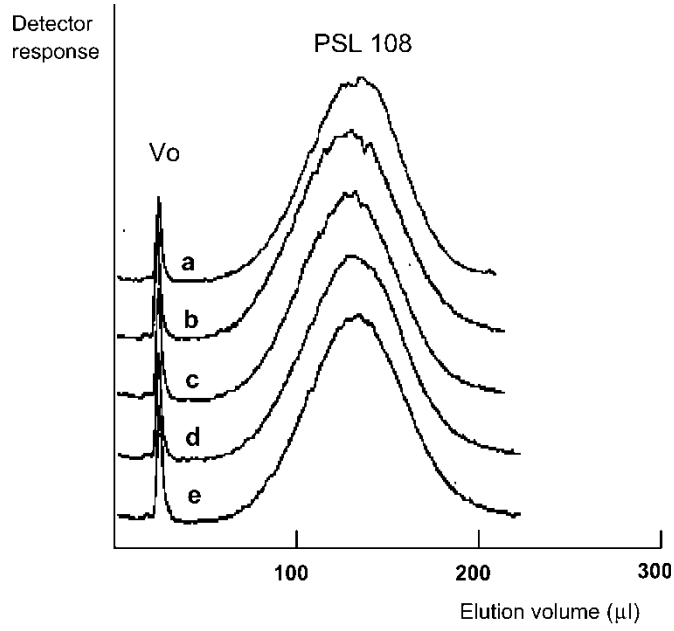

Figure 4. Five of ten fractograms of the polystyrene latex PSL 155 obtained in the laboratory of ULR[b].

Table 2. Statistical evaluation of the results obtained in two participating laboratories

Sample	$\bar{R}$	$\bar{\lambda}$	SD $\bar{\lambda}$	SD $\bar{\lambda}$ (%)	$\bar{\sigma}_N$	SD $\bar{\sigma}_N$	SD $\bar{\sigma}_N$ (%)
Laboratory at UTB							
PSL 108	0.181	0.0323	0.00089	2.8	1.21	0.051	4.2
PSL 155	0.114	0.0198	0.00014	0.7	1.76	0.010	5.7
Average value UTB				1.8			5.0
Laboratory at ULR							
PSL 108	0.171	0.0304	0.00074	2.4	1.24	0.056	4.5
PSL 155	0.133	0.0234	0.00070	3.0	1.39	0.079	5.6
Average value ULR				2.7			5.1
Average value UTB + URL				2.2			

Explanations:
$\bar{R}$ = mean value of the retention ratio calculated by using Eq. (11).
$\bar{\lambda}$ = mean value of the parametr λ calculated by using $\bar{R}$ value and Eq. (2).
σ_N = mean value of standard deviation calculated by using Eq. (13).
SD = standard deviation of the concerned parameter.
SD (%) = standard deviation of the concerned parameter in % of the mean value.

Downloaded At: 17:59 23 January 2011

particles. Correspondingly, the mean normalized standard deviation $\bar{\sigma}_N$, was calculated from:

$$\overline{\sigma_N} = \frac{\sum_1^n \sigma_N}{n} \tag{13}$$

It follows from the data in Table 2 that the precision (repeatability) of the $\bar{\lambda}$ value calculated from the mean retention ratio $\bar{R}$ obtained in a single laboratory lies between 1 and 3%, relative. As a result, with respect to the linear relationship between the retention parameter λ and the particle diameter d_p (see Eq. (8)), the average particle diameter can be determined with as a high precision as 1%, relative. As far as it can be found in the literature,[19,20] no other method of particle size analysis can provide the results of a comparable precision.

However, a small but systematic increase in retention of PSL samples with time was observed. Such an increase in retention (decrease in the retention ratio R) observed for a series of consecutive analyses carried out within one day and repeated after a few days, is shown in Figure 5. This effect could partly be attributed to a partial adsorption of the particles on the accumulation wall. As a result, the adsorbed particles could cause an increase in the frictional drag of the particles retained in subsequent experiments and, consequently, an increase in their retention. Nevertheless, this effect, sometimes described in the literature,[12] is not really supported by the observation that the retention ratio in Figure 5 does not vary systematically and significantly for a series of measurements performed in one laboratory during one day. An alternative explanation can be based on the progressive deterioration of the stability of PSL stock suspension prepared for several

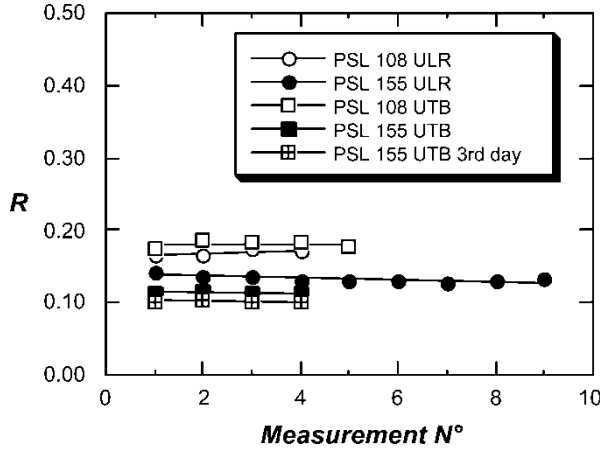

Figure 5. Variation of the retention ratio R of polystyrene latexes PSL 108 and PSL 155 measured in two laboratories. Each measurement series was performed within one day.

Downloaded At: 17:59 23 January 2011

injections and, thus, some kind of aging of the studied samples. This hypothesis is supported by the fact that the retention ratio of the PSL 155 sample changed for a series of measurements carried out with the same stock sample suspension after 3 days of stocking (see Figure 5). The appearance of the opalescence of the carrier liquid was observed if stored one week or more, thus exhibiting also some aging.

In order to verify whether the PSL "aging" hypothesis is correct, three PSL 108 suspensions were prepared by diluting the original PSL standard at different times, stored for 1 week, 6 weeks, and freshly prepared, and then measured by micro-TFFF in one day starting with the oldest suspension and finishing with the fresh one. The results decisively confirmed that the oldest PSL 108 exhibited the highest retention, while the fresh suspension the lowest one. Thus, the "aging" of the suspensions was confirmed. It has to be stressed that the channel was not cleaned before this series of measurements although several samples of PSL 108 and PSL 155 were measured before. Consequently, higher retentions of the aged suspensions cannot be attributed exclusively to the adsorption on the accumulation wall of the particles from previous injections and then to an increase in the frictional drag of the particles retained in subsequent experiments, even if such an adsorption can exist and imposes the need to clean the channel after several analyses, as mentioned above.

Downloaded At: 17:59 23 January 2011

The observed aging effect must have some kind of physical or chemical origin. It might be the variation of surface electrical charges and then the variation of the zeta potential that results in variation of particle-particle or particle-accumulation wall interactions. As a matter of fact, the zeta potential, measured for the diluted PSL 108 suspensions which were stored for several weeks and freshly prepared, progressively decreased for lasting suspensions. The corresponding data are given in Table 3. A substantial but predictable decrease in zeta potential was also found for the PSL 108 sample diluted with a 3 mM NaCl solution. This decrease is caused by the screening of the electrical double-layer of the PSL particles. A substantial but less predictable decrease in zeta potential was found for the PSL sample

Table 3. Variation of zeta potential and average particle size measured by QELS as a function of aging of polystyrene latex suspension

Sample	Mean particle diameter (nm)	Zeta-potential (mV)
PSL 108 original	105	−47.2
PSL 108 fresh	104	−45.3
PSL 108 1 day old	103	−44.3
PSL 108 2 weeks old	98	−35.7
PSL 108 6 weeks old	99	−29.0
PSL 108 saccharose	(140)	−26.2
PSL 108 3 mM NaCl	93	−20.5

diluted with an electrically inactive saccharose solution. A decrease of average particle size measured by QELS could, in principle, be anticipated too because of increased freedom in diffusivity of the particles of lower electrical charges. However, the observed differences given in Table 3 are within the limits of experimental errors (5% at best) of the QELS measurements. The only exception represents the result for the PSL 108 sample measured in the saccharose solution but, in this case, the correction for the increase in viscosity of the solution was not taken into account, which explains the higher value of average particle diameter.

Nevertheless, it is obvious that the best results are obtained if all experiments are performed with maximum care including the periodic cleaning of the micro-TFFF channel and the use of freshly prepared carrier liquid, as well as of sample suspension to be analyzed.

The repeatability of the width of the fractograms is somewhat lower, roughly 5%, relative. This is a consequence of higher signal to noise ratio at both extremes of the fractograms. A conclusion, with regard to the precision of the PSD that might be calculated from the fractogram width, is difficult because the raw fractogram contains not only the information on PSD but also on the contribution of the band broadening. The band broadening, which is due to the dispersive processes mainly inside the separation channel, is influenced by the linear velocity of the carrier liquid and by the relaxation processes. These problems are out of the scope of this paper and will be studied separately. However, the high separating power of micro-TFFF was already demonstrated in a previous paper[7] where the micro-TFFF, hydrodynamic chromatography, scanning electron microscopy, and QELS were compared. Only the micro-TFFF provided a high resolution result.[7] In order to demonstrate this high resolution, the separation of the PSL 108 and PSL 155 in a mixture is shown in Figure 6. The experimental conditions were the same as in repeatability studies described above with the exception of a lower flow rate of 1.67 μL/min. The time of the analysis in this case was relatively long (more than 2 hours), however, no other known method can provide such a high resolution.[19,20] Obviously, if the need to obtain an analytical result in few minutes is imperative, the highest resolution must be sacrificed, which is a general rule for most of the dynamic separation methods.

The stability of the operational variables, such as the temperature of the cold wall T_c, temperature drop between the cold and hot walls ΔT, and the flow rate of the carrier liquid, are the crucial parameters influencing the repeatability of the analytical results. The experimental observation of the temperature stability measured on the micro-TFFF channels used in this study showed that maximum fluctuation of the T_c during the experiments is of the order ± 0.1 K and maximum fluctuation of the ΔT is of the order ± 0.2 K. It means that the stability of the T in Eq. (7) is always largely below 1% and the stability of the ΔT is better than 1% if the temperature drop is higher than $\Delta T = 20$ K. The stability of the flow rate of the syringe type pump

Downloaded At: 17:59 23 January 2011

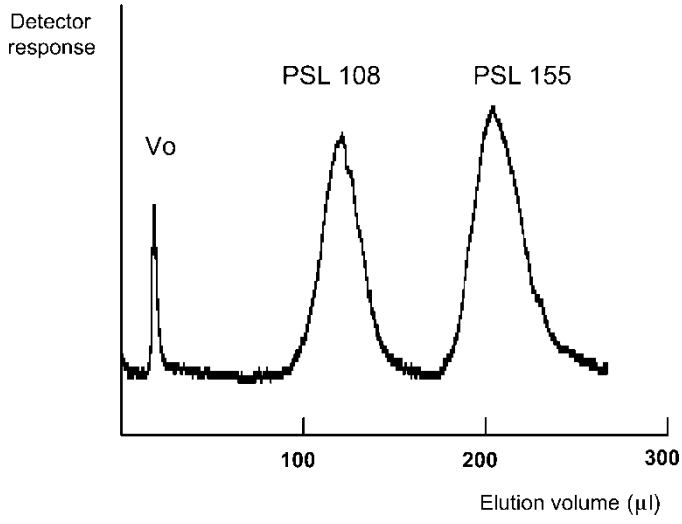

Figure 6. High-resolution micro-TFFF separation of a mixture of the polystyrene latexes PSL 108 and PSL 155.

Downloaded At: 17:59 23 January 2011

equipped with a special stainless steel syringe and used in our studies was tested in a separate experiment, and confirmed the supplier's data, better than 1%, relative within the whole range of the possible flow rates.

In order to determine how the noise (no matter what is its origin) of an experimental fractogram influences the analytical result in terms of the retention ratio R and, consequently, the average particle diameter, as well as standard deviation of the fractogram and, consequently, the width of the PSD, the apparently best fractogram of the PSL 108 standard (fractogram "*e*" on Figure 2) and apparently the worst fractogram of the PSL 155 (fractogram "*h*" on Figure 3) were chosen and treated by different procedures. The retention ratio R was calculated numerically by using the relationship:

$$R = \frac{V_{0,\max}}{\sum_1^n (V_i h_i) / \sum_1^n h_i} \tag{14}$$

where V_i and h_i lying within the zone of the retained species. Standard deviations σ_N were calculated from the raw fractograms "*e*" and "*h*" and from the smoothed fractograms "*e*" and "*h*" by using Eq. (12) For the smoothing of the raw fractograms, the UN-SCAN-IT GEL^{TM} software was applied. The retention ratio $R_{\max}$ corresponding to the maxima of the fractograms, and the standard deviations σ_N were also determined graphically from the raw fractograms "*e*" and "*h*". In such a case, the width of the fractogram (determined as the section of the baseline with the tangents at the inflexion points) corresponds to $4\sigma_N$. All thus obtained data are given in Table 4. It follows from Table 4 that the difference between the results obtained from

Table 4. Comparison of the results obtained by different methods of data treatment

Sample/fractogram	R from Eq. [14]*	σ_N from Eq. [12]*
PSL 108/e-raw	0.176*	1.13*
PSL 108/e-smooth	0.177*	1.12*
PSL 108/e-raw graphical treatment	0.173	1.19
PSL 155/h-raw	0.133*	1.51*
PSL 155/h-smooth	0.133*	1.55*
PSL 155/h-raw graphical treatment	0.136	1.40

the raw and smoothed "higher quality" fractogram "*e*" is negligible. There is even no difference between the data obtained from the raw and smoothed "lower quality" (noised) fractogram "*h*". A simple graphical evaluation of the data provided the results, which are not substantially different in comparison with the results obtained by more accurate numerical treatment.

Downloaded At: 17:59 23 January 2011

CONCLUSIONS

The first experimental investigation of the repeatability of the analytical results concerning the determination of the PSD of colloidal particles by micro-TFFF showed that it is possible to achieve the precision on the level of 1%, relative even under the most critical conditions with a low temperature drop $\Delta T = 30$ K at which the variation of 0.2 K alone (which is roughly the technical limit of the recent apparatus for micro-TFFF) can produce the experimental error of almost 1%. Hopefully, with the use of higher ΔT and some future technical amelioration of the temperature control even higher precision

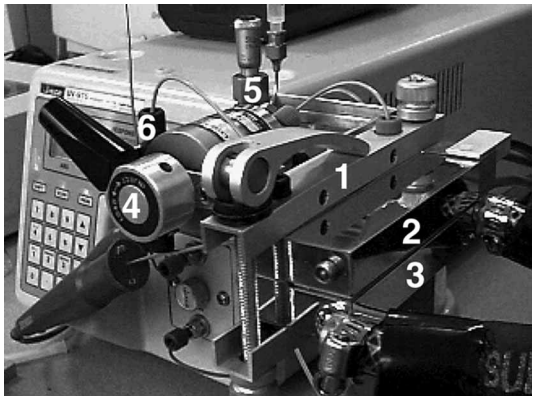

Figure 7. Commercialized micro-TFFF versatile channel unit MicroFrac Compact: Separation channel clamped between two support bars (1); heater (2); cooler (3); injection valve (4); inlet graduated micro-splitter valve (5); outlet micro-metering valve (6).

can be achieved. Such a technical evolution is fully realized by taking into account the progress achieved only during the last three years concerning the construction of the micro-TFFF channel, whose version 2005 is in Figure 7, and can be compared with the model 2002 presented previously.[7]

With regard to the applications of micro-TFFF already performed,[21,22] it is obvious that this new technique is the most universal one in comparison with other techniques of FFF. It is well suited for the analytical separation and characterization not only of the polymers in solution but also of the colloidal nanometer sized particles in suspension as well as micrometer sized particles, without any modification of the separation channel.[21,22] The chemical resistance of the channel allows one to use organic as well as water based solvents in a large range of pH and temperatures.

REFERENCES

Downloaded At: 17:59 23 January 2011

1. Giddings, J.C. A new separation concept based on a coupling of concentration and flow nonuniformities. Separ. Sci. **1966**, *1*, 123–125.
2. Thompson, G.H.; Myers, M.N.; Giddings, J.C. An observation of a field-flow fractionation effect with polystyrene samples. Separ. Sci. **1967**, *2*, 797–800.
3. Giddings, J.C.; Myers, M.N.; Janča, J. Retention characteristics of various polymers in thermal field-flow fractionation. J. Chromatogr. **1979**, *186*, 37–44.
4. Podzimek, S. Round robin test on the molecular characterization of epoxy resins by liquid chromatography. Int. J. Polym. Anal. Charact. **2004**, *9*, 305–316.
5. Just, U.; Weidner, S.; Kilz, P.; Hofe, T. Polymer reference materials: Round-robin tests for determination of molar masses. Int. J. Polym. Anal. Charact. **2005**, *10*, 225–243.
6. Janča, J. Micro-channel thermal field-flow fractionation: New challenge in analysis of macromolecules and particles. J. Liq. Chromatogr. & Rel. Technol. **2002**, *25*, 683–704.
7. Janča, J.; Berneron, J.-F.; Boutin, R. Micro-thermal field-flow fractionation: New high-performance method for particle size distribution analysis. J. Colloid Interface Sci. **2003**, *260*, 317–323.
8. Liu, G.; Giddings, J.C. Separation of particles in nonaqueous suspensions by thermal-electrical field-flow fractionation. Anal. Chem. **1991**, *63*, 296–299.
9. Shiundu, P.M.; Giddings, J.C. Influence of bulk and surface composition on the retention of colloidal particles in thermal field-flow fractionation. J. Chromatogr. A **1995**, *715*, 117–126.
10. Jeon, S.J.; Schimpf, M.E.; Nyborg, A. Compositional effects in the retention of colloids by thermal field-flow fractionation. Anal. Chem. **1997**, *69*, 3442–3450.
11. Mes, E.P.C.; Tijssen, R.; Kok, W.Th. Influence of the carrier composition on thermal field-flow fractionation for the characterisation of sub-micron polystyrene latex particles. J. Chromatogr. A **2001**, *907*, 201–209.
12. Shiundu, P.M.; Munguti, S.M.; Ratanathanawongs Williams, S.K. Practical implications of ionic strength effects on particle retention in thermal field-flow fractionation. J. Chromatogr. A **2003**, *984*, 67–79.
13. Giddings, J.C. Displacement and dispersion of particles of finite size in flow channels with lateral forces. Field-flow fractionation and hydrodynamic chromatography. Sep. Sci. Technol. **1978**, *13*, 241–254.

14. Janča, J.; Ananieva, A. Micro-thermal field-flow fractionation in the characterization of macromolecules and particles: Effect of the steric exclusion mechanism. e-Polymers **2003**.
15. Janča, J.; Ananieva, I.A.; Menshikova, A.Yu.; Evseeva, T.G.; Dupák, J. Effect of channel width on the retention of colloidal particles in polarization, steric, and focusing micro-thermal field-flow fractionation. J. Chromatogr. A **2004**, *1046*, 167–173.
16. Brimhall, S.L.; Myers, M.N.; Caldwell, K.D.; Giddings, J.C. Study of temperature dependence of thermal diffusion in polystyrene/ethylbenzene by thermal field-flow fractionation. J. Polym. Sci., Polym. Phys. Ed. **1985**, *23*, 2445–2456.
17. Janča, J. Micro-thermal field-flow fractionation: New challenge in experimental studies of thermal diffusion of polymers and colloidal particles. Phil. Mag. **2003**, *83*, 2045–2058.
18. Janča, J.; Dupák, J. Elimination of edge effects in micro-thermal field-flow fractionation channel of low aspect ratio by splitting the carrier liquid flow into the main central stream and the thin stream layers at the side channel walls. J. Chromatogr. A **2005**, *1068*, 261–268.
19. Myers, R.A. Ed., *Encyclopedia of Analytical Chemistry*; J. Wiley & Sons, Ltd., 2000.
20. Wilson, I.A., Adlard, T.R., Poole, C.F., Cook, M., Eds., *Encyclopedia of Separation Science*; Academic Press, 2000.
21. Janča, J. Polarization, steric, and focusing micro-thermal field-flow fractionation principles, theory, instrumentation, and applications in polymers and particles analysis. Anal. Chim. Acta **2005**, *540*, 187–196.
22. Janča, J. Micro-thermal field-flow fractionation in the analysis of polymers and particles: A review. Int. J. Polym. Anal. Charact. **2006**, *11*, 57–70.

Received July 24, 2006
Accepted August 23, 2006
Manuscript 6919

Downloaded At: 17:59 23 January 2011